ELSEVIER

Biochimica et Biophysica Acta 1457 (2000) 1–17

BIOCHIMICA ET BIOPHYSICA ACTA

BBA

www.elsevier.com/locate/bba

Escape probability and trapping mechanism in purple bacteria: revisited

Karen Bernhardt, Hans-Wilhelm Trissl *

Abteilung Biophysik, Fachbereich Biologie/Chemie, University of Osnabrück, Barbarastr. 11, D-49069 Osnabrück, Germany

Received 25 May 1999; accepted 8 November 1999

Abstract

Despite intensive research for decades, the trapping mechanism in the core complex of purple bacteria is still under discussion. In this article, it is attempted to derive a conceptionally simple model that is consistent with all basic experimental observations and that allows definite conclusions on the trapping mechanism. Some experimental data reported in the literature are conflicting or incomplete. Therefore we repeated two already published experiments like the time-resolved fluorescence decay in LH1-only purple bacteria *Rhodospirillum rubrum* and *Rhodopseudomonas viridis* chromatophores with open and closed (Q_A^-) reaction centers. Furthermore, we measured fluorescence excitation spectra for both species under the two redox-conditions. These data, all measured at room temperature, were analyzed by a target analysis based on a three-state model (antenna, primary donor, and radical pair). All states were allowed to react reversibly and their decay channels were taken into consideration. This leads to seven rate constants to be determined. It turns out that a unique set of numerical values of these rate constants can be found, when further experimental constraints are met simultaneously, i.e. the ratio of the fluorescence yields in the open and closed (Q_A^-) states $F_m/F_o \approx 2$ and the P^+H^--recombination kinetics of 3–6 ns. The model allows to define and to quantify escape probabilities and the transfer equilibrium. We conclude that trapping in LH1-only purple bacteria is largely transfer-to-the-trap-limited. Furthermore, the model predicts properties of the reaction center (RC) in its native LH1-environment. Within the framework of our model, the predicted P^+H^--recombination kinetics are nearly indistinguishable for a hypothetically isolated RC and an antenna-RC complex, which is in contrast to published experimental data for physically isolated RCs. Therefore RC preparations may display modified kinetic properties.

Keywords: Fluorescence decay kinetics; Fluorescence excitation spectrum; Fluorescence yield; Modeling; Trapping mechanism

1. Introduction

The core of the photosynthetic unit of purple bacteria consists of a reaction center (RC) surrounded by a light harvesting complex (LH1) (for review see [1]). Two different trapping mechanisms in the LH1-RC core complexes of purple bacteria are currently discussed. These are (1) the transfer-to-the-trap-limited and (2) the trap-limited (or RC-controlled) mechanisms. The trapping process is said to be transfer-to-the-trap-limited if the transfer from the antenna to the primary donor is rate-limiting and trap-limited if the primary charge separation in the RC is rate-limiting. On the one hand, there is kinetic and

Abbreviations: BChl, bacteriochlorophyll; PSU, photosynthetic unit; RC, reaction center; TMPD, *N*,*N*,*N*′,*N*′-tetramethyl-*p*-phenylenediamine; LH1, light harvesting complex 1; LH2, light harvesting complex 2

* Corresponding author.

0005-2728/00/$ – see front matter
PII: S0005-2728(99)00103-6

structural evidence in favor of transfer-to-the-trap-limited mechanism which has been reviewed by several authors [2–4] and on the other, the RC-controlled trapping mechanism has been suggested by Müller et al. [5] and Borisov [6].

The ring-shaped arrangement of the antenna bacteriochlorophylls (BChl) molecules at a distance of 42 Å around the RC intuitively suggests the transfer-to-the-trap-limited mechanism [1,7]. However, the similar absorption maxima of LH1 and the primary donor (P) in connection with the abundance of B880 antenna pigments argues for a much faster backward than forward transfer, suggesting a high escape probability towards the antenna for an exciton residing on P. In the case of *Rhodopseudomonas viridis* the absorption maximum of the antenna (1015 nm) is even more red than that of P (980 nm [8,9]) suggesting an even higher escape probability. The matter is, however, more complicated due to the competitive fast decay channel for P*, the primary charge separation, and clarification requires a quantitative analysis.

In chromatophores of different purple bacteria with open RCs, the escape probability seems to be small, but also higher escape probabilities have been reported: specifically for *Rhodopseudomonas sphaeroides* R26, *Rsp. viridis*, *Rhodospirillum rubrum* and *Chromatium tepidum* $\leq 2\%$ [10], for a LH2-less mutant of *Rhodobacter capsulatus* $15 \pm 10\%$ [11], for *Rps. viridis* 50% [12], $20 \pm 5\%$ [13] and $\leq 2\%$ [8], for *Rs. rubrum* $25 \pm 5\%$ [14], and for *Chromatium minutissimum* 10–20% [15]. These data do not allow to derive a clear picture. Unfortunately, different definitions of the term 'escape probability' have been used in the literature, and the escape probability in reduced systems (LH1-RC(Q_A^-)) has not yet been considered. Therefore, the quantitative analysis of a comprehensive, but simple model is needed to decide on the escape probabilities and trapping mechanism.

The results from time resolved measurements are similarly confusing. Dominating phases in the fluorescence decay and absorption change kinetics from various LH1-only purple bacteria with open RCs range from 50 to 82 ps [12,14,16–21], whereas with closed (Q_A^-) RCs the decay is biphasic with again a 60–90 ps phase and a ≈ 2 ns phase [14,18,20,22]. The time constant of the fast phase is usually considered to represent the trapping time. A dependence of the trapping time on the redox state (open or closed (Q_A^-)) of the RC has been reported for *Rb. sphaeroides* [5], *Rs. rubrum* [22] and *Rsp. viridis* [12]. This would argue for the RC-controlled mechanism. An independence of the trapping time of the redox state (open or closed (Q_A^-)) has been reported for *Rsp. viridis* [23] which argues for the transfer-to-the-trap-limited mechanism.

An exhaustive analysis of the kinetic data should include other experimental facts. For example, the well established ratio of fluorescence yields for chromatophores or membranes with closed (Q_A^-) and open RCs of approximately two [24,25] must be met. Also the escape probabilities as assayed by fluorescence excitation spectra must be correctly predicted, as well as the P^+H^--recombination kinetic. Furthermore, the dependence of the charge separation time on the redox-state of the RC (2.3–3.5 ps for open [26–28] and about 6 ps for closed (Q_A^-) [29]) has also to be taken into account.

A possible source of these partially conflicting experimental data might be different properties of the RC embedded in either natural membranes or in detergent micelles. Different P^+H^--recombination kinetics in chromatophores and RC preparations have been published [30,31]. As a possible cause the authors propose the presence or absence of antenna pigments. The effect may be based on two different mechanisms: one possibility is the additional decay path due to efficient exciton backtransfer to the antenna. A second possibility is an influence of the LH1 complex on the energetics (ΔG^0) of primary charge separation [32].

To clarify some of the experimental inconsistencies we re-measured the fluorescence decay kinetics and fluorescence excitation spectra of two LH1-only purple bacteria, namely *Rs. rubrum* and *Rps. viridis*, in two redox-states. The aim of the present study is to find a minimal model that is able to account for these data as well as for the ratio of fluorescence yield F_m/F_o [24,25] and the P^+H^--recombination kinetics [30,31], using the latter as constraints. The constraints allow to determine all rate constants of the model.

A mathematical exact definition of the escape probability requires a model or kinetic scheme. Our minimal model offers the possibility to quantify different conceivable escape probabilities for *Rs. rubrum*

and *Rsp. viridis*. The experimental meanings and the practical advantages of the different definitions will be discussed.

We conclude that trapping in LH1-only purple bacteria is essentially transfer-to-the-trap-limited.

2. Materials and methods

Rs. rubrum and *Rsp. viridis* were anaerobically cultured according to Drews [33] and chromatophores were prepared according to Otte et al. [10]. The chromatophores or membranes were diluted in 10 mM Tris, pH 7.4 for *Rs. rubrum* and pH 8.0 for *Rsp. viridis*. To keep all RCs open 20 μM TMPD (*Rs. rubrum*) or 50 μM TMPD (*Rsp. viridis*) together with 10 mM ascorbate were used. The quinone acceptor Q_A was reduced by 10 mM dithionit.

Fluorescence decay kinetics measurements were performed with an analog single-shot detection device described by Trissl and Wulf [34]. The excitation source was a Nd-YAG laser emitting 30 ps pulses at 532 nm. All kinetic traces were the average of 20 events collected at a repetition rate of 0.3 Hz. The absorption in the 0.1 mm cuvette for *Rs. rubrum* at 900 nm was 0.28, for *Rsp. viridis* at 1040 nm 0.113. The fluorescence from *Rs. rubrum* was detected in the range of 770–1100 nm and from *Rsp. viridis* in the range of 1000–1100 nm. The kinetic data were analyzed by convoluting the kinetics calculated for a three-state model with the response function of the apparatus and minimizing the sum of the squared residuals by varying the parameters of the model under the condition of meeting other experimental constraints. The response function was obtained by recording the 0.5 ps fluorescence decay kinetics from purple membranes.

Fluorescence excitation spectra were measured with a custom-built setup. The excitation source was a 20 μs Xenon flash operated at a repetition rate of 1 Hz. The excitation light was passed through a long-pass filter (OG 550) before it entered a monochromator (Spex) with a Blaze-wavelength of 750 nm. The slit widths were 1.25 mm at the entrance and exit. A cuvette with an inner sectional area of 2×10 mm was used (10 mm at excitation, 2 mm at emission). The flash energy at 600 nm was approximately 4×10^{-8} J/cm^2 at the front of the cuvette. This corresponds to approximately 2×10^{-4} hits per PSU. The absorption of *Rs. rubrum* at 900 nm was 0.09, and that of *Rsp. viridis* membranes at 1040 nm, 0.07. The emission was detected at 930 ± 5 nm for *Rs. rubrum* and at $\geq$1000 nm for *Rsp. viridis* under an angle of 90° with an Avalanche Photodiode (EG&G; model C30626E).

Absorption spectra were measured with an SLM-Aminco DW2000 spectrophotometer equipped with a Si-avalanche photodiode as detector.

All measurements were performed at room temperature.

3. Results

3.1. The model used for analysis

To describe the essentials of the trapping process in the PSU of LH1-only purple bacteria with either open or closed (Q_A^-) RCs we tested a minimal reaction scheme (Scheme 1) consisting of three states: (1) the excited state on one of the antenna pigments A*; (2) the excited state on the primary donor P*; and (3) the radical pair state RP. Y stands for the charge stabilized state (or product yield) in open RCs. Non-photochemical losses in the antenna and on the primary donor are accounted for by the same rate constant k_ℓ. Excitons can travel back and forth between A and P with the rate constants for trapping k_t and detrapping k_{-t}. These two rate constants describe a photophysical process that, for obvious reasons, is independent of the redox state of Q_A. The charge separation occurs with the rate constant k_1, the back-reaction (radiative charge recombination) with $k_{-1}^{o,c}$ in the open and closed states. The radical pair decays radiationless with the rate constant k_d. This rate constant accounts for the transition into the ground state and the ^{3}P triplet state. The contribution of the latter is small [35] and will not further be discussed. The product Y ($P^+Q_A^-$) in the open state is

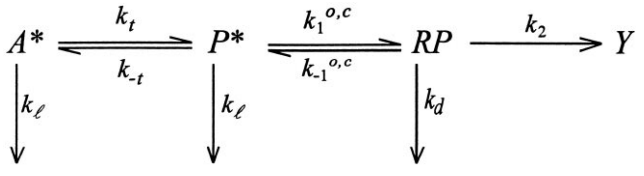

Scheme 1.

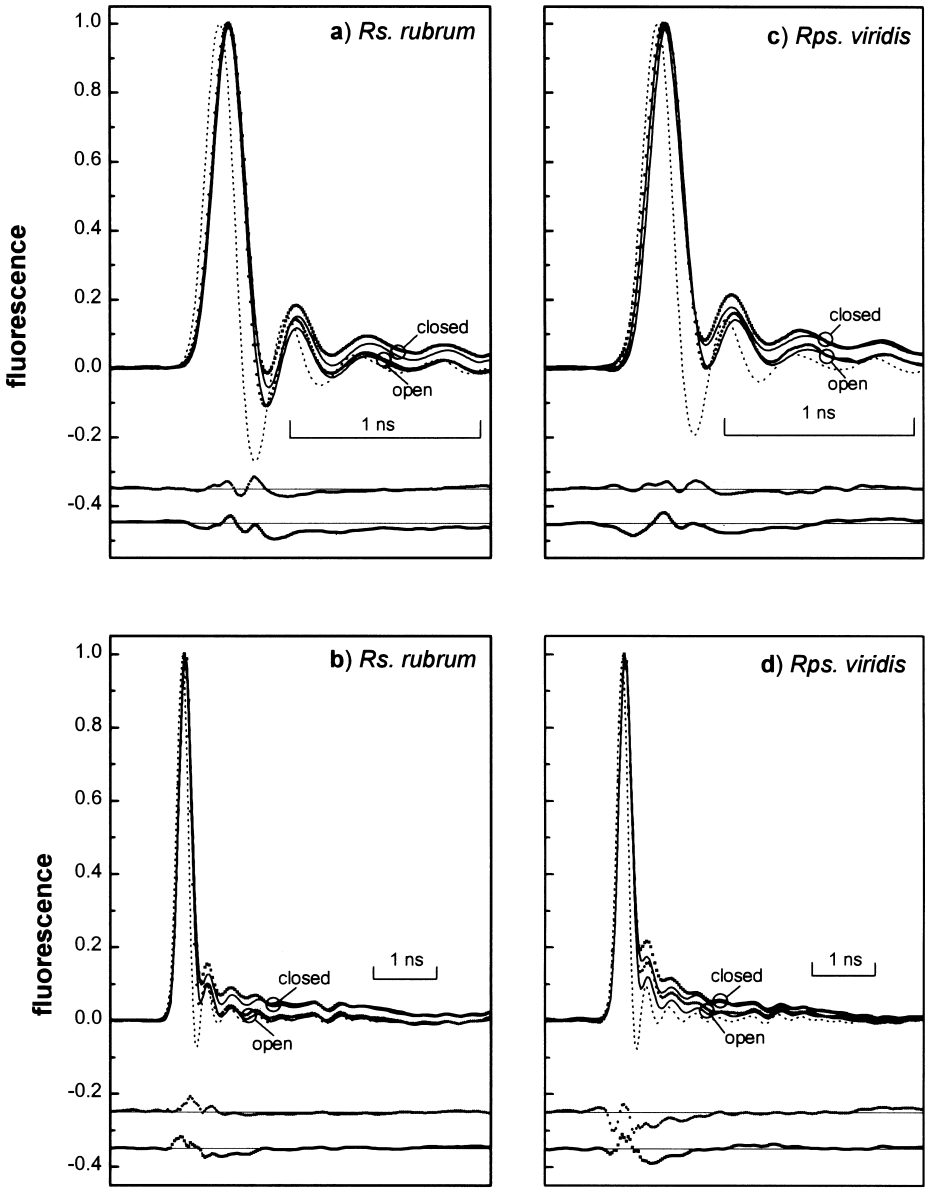

Fig. 1. Fluorescence signals (dots) from chromatophores of *Rs. rubrum* (a,b) and *Rps. viridis* (c,d) recorded on different time bases as indicated. Signals for open RCs always lie below signals for closed (Q_A^-) RCs. The response functions are indicated by short dashes. Beneath each fluorescence signal are shown the residuals of best fit curves (solid lines) and the data. The upper residuals refer to the open state and the lower ones to the closed state. The best fit parameters are listed in Tables 1 and 2.

assumed to be irreversibly formed with the rate constant k_2. For the closed (Q_A^-) state Y is not formed ($k_2 = 0$). Open and closed (Q_A^-) RCs differ by the rate constant for charge separation $k_1^{o,c}$ and the presence or absence of the charge stabilization step (k_2). All other reaction paths and rate constants are set the same for the open and closed (Q_A^-) state (Scheme 1).

The rate constant k_ℓ includes all other deactivation processes than the indicated ones (like the emission by fluorescence k_{rad}). We assumed k_{rad} of A and P to be the same, if not otherwise stated. The mathematical treatment of the scheme and the various solutions are given in the Appendix A.

3.2. Fluorescence decay kinetics

Fig. 1a and b show fluorescence signals (dots) from chromatophores of *Rs. rubrum* with open and

Table 1
Assumed parameters for the model calculations taken from the literature

	Rs. rubrum	*Rsp. viridis*
No. of antenna BChl N_A	32	24
No. of primary donor BChl N_P	2	2
Absorption maximum of antenna λ_A^{max}	881 nm	1013 nm
Absorption maximum of primary donor λ_P^{max}	880 nm	980 nm
Stokes shift of antenna S_A	200 cm^{-1}	200 cm^{-1}
Stokes shift of primary donor S_P	550 cm^{-1}	550 cm^{-1}
Rate constant of primary charge separation in open RCs k_1^o	$(2.4\ ps)^{-1}$	$(2.4\ ps)^{-1}$
Rate constant of primary charge separation in closed RCs k_1^c	$(4.8\ ps)^{-1}$	$(5.0\ ps)^{-1}$
Rate constant for antenna losses k_ℓ	$(700\ ps)^{-1}$	$(700\ ps)^{-1}$

closed (Q_A^-) RCs acquired on different time bases. These signals result from the exponential fluorescence decay kinetics convoluted by the detector response function (Fig. 1a–d, short dashes). Also shown are the fits (solid lines) to the signals. In the lower parts each figure contains the residuals of the fits that were obtained with the parameters listed in Tables 1 and 2. The signals from *Rsp. viridis* membranes (Fig. 1c,d) were analyzed analogously.

The kinetic traces in Fig. 1 for *Rs. rubrum* were fitted by a target analysis [36] which took into account the constraints $F_m/F_o \approx 2$ [24] and P^+H^--recombination kinetics of about 5 ns as in *Rb. sphaeroides* [30]. We used for fitting directly the molecular rate constants of the model depicted in Scheme 1. The rate constants for trapping, k_t, charge recombination to P*, $k_{-1}^{o,c}$, and radiationless charge recombination, k_d, were fit parameters, whereas the rate constants for antenna losses, k_ℓ, and primary charge separation, $k_1^{o,c}$, the antenna size (N_A), the number of BChls forming the primary donor (N_P), the absorption maxima of the antenna, (λ_A^{max}), or P, (λ_P^{max}), and their Stokes shifts S_A and S_P were fixed. Their values (see Table 1) were taken from the literature: $k_\ell = (700\ ps)^{-1}$ [37], $k_1^o = (2.4\ ps)^{-1}$ [26–28], $k_1^c \approx 0.5 \cdot k_1^o$ [29], $N_A = 32$ [7,38], $\lambda_A^{max} = 881$ nm, $\lambda_P^{max} = 880$ nm, $S_A = 200\ cm^{-1}$ and $S_P = 550\ cm^{-1}$ [39]. The values of the fit parameters (see Table 2) that described reasonably well the kinetic data and fulfilled the constraints are: $k_t = (69.3\ ps)^{-1}$, $k_{-t} = (24.2\ ps)^{-1}$, $k_{-1}^c = (0.9\ ns)^{-1}$, $k_2 = (220\ ps)^{-1}$, $k_d = (5.7\ ns)^{-1}$. The value for k_{-1}^o can be varied within a factor of two with respect to k_{-1}^c without markedly effecting the residuals. Dropping the constraints in the analysis of the kinetic data leads to improved residuals.

In the case of *Rps. viridis* membranes (Fig. 1c,d) with solely open RCs the target analysis with Scheme 1 gave unsatisfactory fits of the kinetics. Satisfactory fits could only be obtained under the assumption that a fraction of RCs was closed or had an unoccupied Q_A binding site. The theoretical curves in Fig. 1c and d were calculated with 75% open and 25% closed RCs. This fraction seems neither to depend on the redox-conditions nor on the repetition rate used for data accumulation. However, we made the observation that in whole cells of *Rps. viridis* the fraction of closed RCs needed for good fits was smaller than in membrane preparations.

3.3. Fluorescence excitation spectra

The fluorescence excitation spectra of *Rs. rubrum* and *Rps. viridis* when all RCs are open and when the

Table 2
Fit parameters resulting of the target analysis of the kinetic data in Fig. 1 and the constrains $F_m/F_o \approx 2$ and the charge recombination time of 5.0–5.4 ns for *Rs. rubrum* and 2.8 ns for *Rsp. viridis*

	Rs. rubrum	*Rsp. viridis*
Rate constant of exciton transfer antenna-primary donor k_t	$(69\ ps)^{-1}$	$(52\ ps)^{-1}$
Rate constant of backreaction for closed RCs k_{-1}^c	$(900\ ps)^{-1}$	$(1.5\ ns)^{-1}$
Rate constant of charge stabilization k_2	$(220\ ps)^{-1}$	$(230\ ps)^{-1}$
Rate constant of decay of the radical pair k_d	$(5.7\ ns)^{-1}$	$(3.15\ ns)^{-1}$

first quinone acceptor is reduced (closed Q_A^-) are shown in Fig. 2a,b (thick dots). The fluorescence excitation spectra were not normalized in order to illustrate the change in the relative quantum yields in response to the different redox states. Also shown are the one minus transmission (1−T) spectra (dotted curves) which were scaled to fit the fluorescence excitation spectra. The ratios of the scaling factors between the open and closed states were 1.9 for *Rs. rubrum* and 1.8 for *Rps. viridis*.

In the case of *Rs. rubrum* the RC absorption band at 800 nm (ascribed to the accessory BChls) is practically lacking in the fluorescence excitation spectra when the RCs are open (Fig. 2a, lower spectrum). This finding, which is in agreement with Otte et al. [10], indicates a small escape probability. However, with closed (Q_A^-) RCs the RC band is very pronounced (Fig. 2a, upper spectrum), indicating a high escape probability. To quantify the observation we split the (1−T) spectrum into an antenna part and the naked RC (Gaussian band at 800 nm) and used the escape probability $p_{esc}^{o,c}$ defined by Eq. A5c, which applies for the total fluorescence yield, i.e. the measured quantity. The escape probabilities (quoted in Table 3) were calculated for open and closed RCs with the parameters in Tables 1 and 2. They are then used as amplitude factors for the RC band which is added to the pure antenna spectrum. The resulting theoretical spectra (open/closed) are shown in Fig. 2 as fits (solid lines). It is worth noting that the RC band of the (1−T) spectrum is still larger than the excitation spectrum under reducing conditions which indicates an escape probability of less than 100%.

The situation is significantly different for *Rsp. viridis*. Here the RC absorption band at 830 nm is rather pronounced in the fluorescence excitation spectra when the RCs are open (Fig. 2b, lower spectrum), indicating a rather high escape probability. This finding is in striking disagreement with Otte et al. [10], who found this band totally lacking. A possible explanation could be the establishment of a different redox state ($P960^+$) in the experiments by Otte et al. due to the approximately 100-fold stronger illumination compared to the one used here.

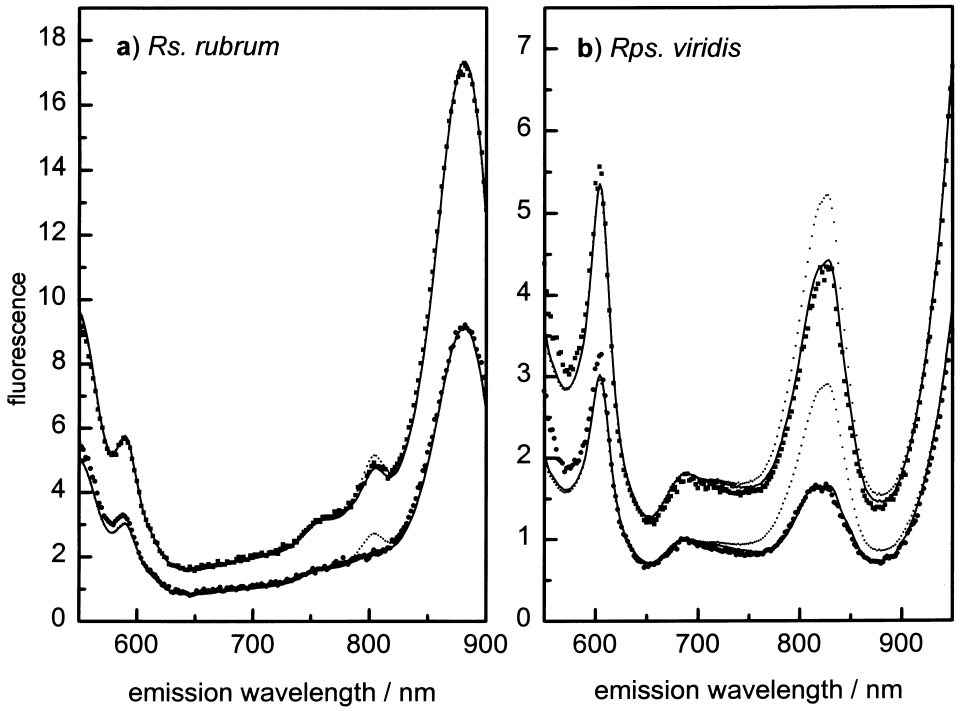

Fig. 2. Fluorescence excitation spectra of (a) *Rs. rubrum* and (b) *Rps. viridis* in two redox-states of the RC (open (circles) and closed (Q_A^-) (squares)). The spectra are not normalized to show the ratios of fluorescence yields which were 1.9 for *Rs. rubrum* and 1.8 for *Rps. viridis*. (1−T) spectra (small dots) corresponding to these ratios are shown for comparison. Theoretical fluorescence excitation spectra (solid lines) were calculated as described in Section 3 using the escape probabilities given in Table 3.

When the RCs were closed (Q_A^-) the RC absorption band increased considerably (Fig. 2b, upper spectrum), indicating a still higher escape probability. This finding would agree with the reported excitation spectra for *Rps. viridis* [10], which were measured at 6 K. The solid lines in Fig. 2b represent the calculated excitation spectra with the escape probabilities listed in Table 3. These spectra agree well with the measured spectra. Under reducing conditions, the RC band in the (1−T) spectrum is still larger than the excitation spectrum as it is the case for *Rs. rubrum*.

4. Discussion

To describe the trapping process in the core complexes of purple bacteria, we assumed a simple reaction scheme consisting of only three transiently formed states and an irreversibly formed product (Scheme 1). One parameter set was searched that is able to predict the measured quantities: (1) fluorescence decay kinetics; (2) fluorescence excitation spectra; (3) ratio of fluorescence yields with open and closed (Q_A^-) RCs; and (4) the P^+H^--recombination kinetics. A unique solution of the parameters was found (Tables 1 and 2) that fulfilled all constraints. We will first discuss the choice of the parameters used with reference to the literature and then draw some general conclusions on the escape probability and the trapping mechanism in the core complexes of purple bacteria.

4.1. Choice of fixed parameters

The antenna size of *Rs. rubrum* was assumed to be $N_A = 32$ [7,38] and the absorption maximum was measured at $\lambda_A^{max} = 881$ nm. For *Rsp. viridis*, N_A was assumed to be $N_A = 24$ [40] and the absorption maximum was measured at $\lambda_A^{max} = 1013$ nm.

We assumed the absorption maximum of the primary donor of *Rs. rubrum* to lie at 880 nm (Table 1). The primary donor of *Rps. viridis*, however, commonly called P960 after its IR absorption band in RC preparations, shows the main bleaching due to the oxidation of the primary donor in membranes at 980 nm [8,9], and we have chosen this wavelength for the model calculations.

The following Stokes shifts of the fluorescent states were taken: for the antenna pigments of both bacteria $S_A = 200$ cm^{-1} (as follows from the wavelength maxima of absorption and fluorescence), and for the primary donor of both RCs types $S_P = 550$ cm^{-1} [39,41].

The primary charge separation in open RCs was assumed to proceed monoexponentially with a rate constant of $(2.4\ \text{ps})^{-1}$. Published time constants range from 1.9 to 5.1 ps [26–28,42–45]. The primary charge separation in closed (Q_A^-) RCs was assumed to be about two-fold slower [29].

The rate constant of charge stabilization in open RCs was chosen $k_2 = (220\text{–}230\ \text{ps})^{-1}$ which is in the order of published values which fall within the range of $(125\text{–}240\ \text{ps})^{-1}$ [19,21,23,28,46,47].

The rate constant for non-photochemical losses, k_ℓ, was chosen to be $(700\ \text{ps})^{-1}$ [37]. Unfortunately, there is no reliable information on the most realistic value. Several other numbers have been used in the literature, ranging from $(640\ \text{ps})^{-1}$ to $(2.3\ \text{ns})^{-1}$ [26,48]. However, the results of our analysis did not change significantly when this parameter was decreased to $(1.1\ \text{ns})^{-1}$.

The other rate constants not mentioned in this section were adjustable fit parameters to our data.

4.2. Trapping times with open and closed (Q_A^-) RCs

A wide range of trapping times in chromatophores or membranes of purple bacteria have been reported [12,14,16–22]. We shall first discuss the BChl *b*-containing *Rps. viridis* and next the BChl *a*-containing *Rs. rubrum*.

The shortest trapping times of 40–45 ps have been deduced from photovoltage measurements on *Rsp. viridis* and have been reported to be independent of the reduction state [23,46]. In contrast, redox state dependent trapping times of 60 ps in the open and 90 ps in the closed (Q_A^-) state have been observed by low intensity picosecond absorption spectroscopy [12]. The origin of this discrepancy is most likely due to high intensity excitation in the former experiments which speeded up the kinetics. Our data in Fig. 1 obtained by fluorescence decay analysis (excitation intensity of ≤ 0.1 excitons per PSU) displayed a 69-ps kinetic phase in the open state and a 91-ps kinetic phase in the closed (Q_A^-) as predicted by the

Table 3
Derived quantities from the parameters in Tables 1 and 2

	Rs. rubrum	*Rsp. viridis*
F_m/F_o	2.18	2.37
Rate constant of exciton transfer primary donor-antenna k_{-t}	$(24.2\ ps)^{-1}$	$(4.6\ ps)^{-1}$
Escape probability p^{o}_{esc}	0.140	0.395
Escape probability p^{c}_{esc}	0.659	0.787
Escape probability p'^{o}_{esc}	0.014	0.042
Escape probability p'^{c}_{esc}	0.148	0.200
Escape probability p''^{o}_{esc}	0.105	0.372
Escape probability p''^{c}_{esc}	0.571	0.767
Photochemical yield	0.863	0.832
Thermodynamic equilibrium constant K	0.349	0.091
Transfer equilibrium constant (open) $\tilde{K}^{o}_{0}$	0.270	0.076
Transfer equilibrium constant (closed (Q_A^-)) $\tilde{K}^{c}_{0}$	0.378	0.096
${}^{A}F^{o}_{P}/({}^{A}F^{o}_{A}+{}^{A}F^{o}_{P})$	0.035	0.033
${}^{A}F^{c}_{P}/({}^{A}F^{c}_{A}+{}^{A}F^{c}_{P})$	0.166	0.065
${}^{P}F^{o}_{P}/({}^{P}F^{o}_{A}+{}^{P}F^{o}_{P})$	0.277	0.089
${}^{P}F^{c}_{P}/({}^{P}F^{c}_{A}+{}^{P}F^{c}_{P})$	0.277	0.089

target analysis (Table 4). These numbers agree reasonably well with the picosecond absorption data [12].

There are several other reports on *Rps. viridis* in which biphasic decays with components in the range of 50–500 ps were measured. We do not discuss these results because it remains unknown whether those samples contained a mixture of open and closed RCs and additionally also RCs in two different closed states (Q_A^- and P^+).

In this context, we note that our parameter sets for both bacteria in the open state predict, in addition to the trapping time, a 210–220-ps phase with $\leq 3\%$ amplitude (Table 4), which is related to the charge stabilization step. In the case of chromatophores with closed (Q_A^-) RCs our parameter set predicts one phase that falls into the 50–500 ps time domain (Table 4). Therefore, in the open as well as in the closed state the fluorescence decay should be essentially monoexponential, given a well-defined redox state and a homogeneous sample.

The dependence of the trapping time on the redox state is a direct consequence of the different rate of the primary charge separation in the RC, $k_1^{o,c}$, which, according to the literature, was assumed for both species to be two-fold slower in closed than in open RCs [26–29].

In contrast to *Rps. viridis*, the trapping kinetics in *Rs. rubrum* did not significantly depend on the redox state of the RC: here the phases were nearly the same with 68 vs. 73 ps (Table 4). This is in contrast to Borisov et al. [22] who found a trapping time of about 60 ps for the open state and about 80 ps in the closed (Q_A^-) state. Faster trapping times reported in the literature [16,17] may be explained by too high excitation densities leading to an accelerated trapping and also to annihilation [49]. The small influence of $k_1^{o,c}$ on the overall trapping time in *Rs. rubrum* found by us is totally consistent with the weak dependence of the trapping time on the primary charge separation in RC mutants of *Rb. sphaeroides* [37].

The molecular rate constant for exciton transfer from the antenna to the primary donor (Table 2) are 69 ps for *Rs. rubrum* and 52 ps for *Rsp. viridis*. These numbers agree perfectly with theoretical calculations for the ring-shaped LH1-RC by Ritz et al. [50].

4.3. Detrapping with open and closed (Q_A^-) RCs

The rate constant for detrapping k_{-t} is directly related to the rate constant for trapping by the energetic Boltzmann term and the entropic degeneracy term for the states (Eq. 1) and therefore k_{-t} is no fit parameter, but belongs to the derived quantities (Table 2). The detrapping rate is given by:

Table 4
Amplitudes (a_1) and (apparent) time constants (τ_1) of fluorescence kinetics for chromatophores and excitation of the antenna calculated with the parameters in Tables 1 and 2

		a_1	τ_1 (ps)	a_2	τ_2 (ps)	a_3	τ_3 (ps)
Rs. rubrum	open	−0.028	2	1.012	68	0.016	214
chromatophores	closed	−0.048	2	1.032	73	0.016	5050
Rsp. viridis	open	−0.020	2	0.988	69	0.033	218
membranes	closed	−0.022	2	0.991	91	0.031	2800
Rs. rubrum	open	0.997	2.3	–	–	0.003	212
RCs	closed	0.995	4.5	–	–	0.005	5501
Rsp. viridis	open	0.998	2.4	–	–	0.002	215
RCs	closed	0.997	4.9	–	–	0.003	3114

In the lower two rows the simulated amplitudes and time constants for RCs and excitation of the primary donor are given.

$$k_{-t} = k_t \cdot \frac{N_A}{N_P} \cdot e^{E_P - E_A} \quad (1)$$

in which N_A denotes the number of degenerated antenna pigments and N_P the number of pigments constituting the special pair primary donor ($N_P = 2$). The energy levels E_A and E_P in Eq. 1 refer to the relaxed electronic states of the antenna and the primary donor, respectively, which we estimated from the absorption maximum and the Stokes shifts, S_A and S_P, according to:

$$E_A = \frac{hc}{\lambda_A^{max}} - S_A \quad (2a)$$

$$E_P = \frac{hc}{\lambda_P^{max}} - S_P \quad (2b)$$

Given the input parameters of Table 1, the detrapping rate constant for *Rs. rubrum* is $(24\ ps)^{-1}$ and for *Rsp. viridis* $(4.6\ ps)^{-1}$. These values are in good agreement with estimations from the literature which range from $(6.5\ ps)^{-1}$ to $(25\ ps)^{-1}$ for different purple bacteria [11,14,51]. According to our parameter set, detrapping is 3-fold (*Rs. rubrum*) and 11-fold (*Rps. viridis*) faster than trapping. Hence, the thermodynamic equilibrium lies clearly on the antenna side. This is also reflected by the thermodynamic equilibrium constants of 0.35 (*Rs. rubrum*) and 0.09 (*Rps. viridis*) which are significantly smaller than one (Table 3). In other words, the residence probability for an exciton lies on the antenna side if a perfect equilibration would occur. However, equilibrium thermodynamics is not the most appropriate approach to describe the highly dynamic antenna-RC system.

4.4. Transfer equilibrium

The question arises to what extent the system deviates from thermodynamic equilibrium and in what time the thermal equilibrium would become established. Whereas the thermodynamic equilibrium constant is defined by $K = k_t/k_{-t}$, the transfer equilibrium constant $\tilde{K}_0^{o,c}$ is given by Eq. A7. The time course with which the transfer equilibrium establishes follows from the ratio of the time-dependent excited states on the primary donor and the antenna, $A(t)$ and $P(t)$ (see Appendix A). Intuitively, the fast depopulation kinetics of P* by the primary charge separation may lead to a significantly smaller concentration of P* than predicted by thermodynamic equilibrium.

The time courses of the ratio of the exciton densities on the primary donor and the antenna are shown in Fig. 3a for the different excitation conditions and redox states of the RC taking the parameter set for *Rs. rubrum*. (The figure for *Rsp. viridis* looks qualitatively very similar.) The time needed to establish the transfer equilibrium as predicted by the model and the rate constants in Tables 1 and 2 is on the order of a few 100 ps (Fig. 3a). One may notice fast ps-transients that correspond to the 2 ps phases listed in Table 4. These are not further discussed here. The initial excitation condition slightly affects

the kinetics with which the transfer equilibria are reached. The transfer equilibrium constants depend on the redox state of the RC, but are independent of the initial excitation. Both constants deviate markedly from the thermodynamic equilibrium constant (Fig. 3a and Table 3).

These deviations indicate that the exciton-radical pair model introduced for PS II does not hold for purple bacteria, since this model assumes the thermodynamic equilibrium between P* and A*. However,

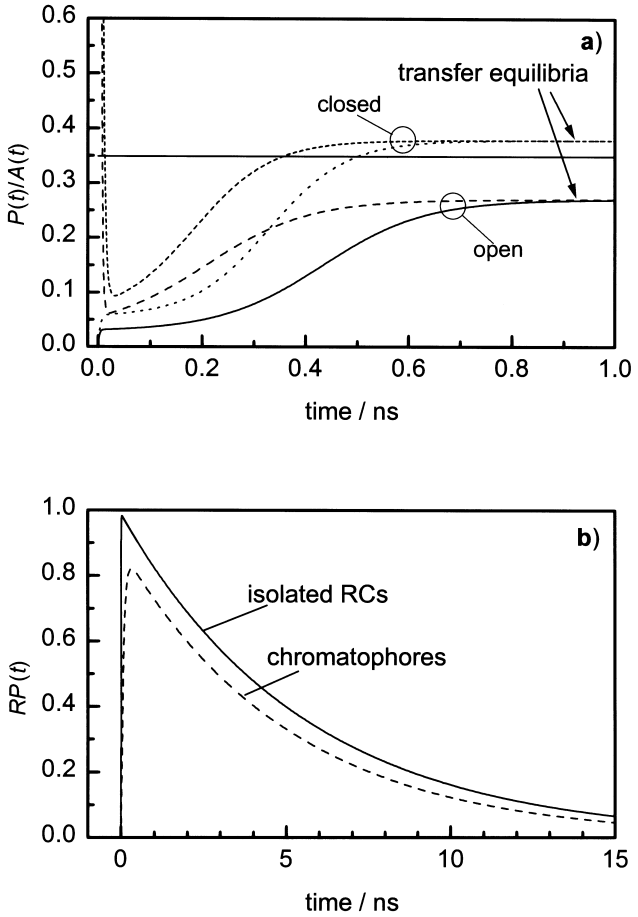

Fig. 3. (a) Time course of the ratio of exciton concentration on P to exciton concentration on A. Horizontal solid line, thermodynamic equilibrium; short dashes, RC in the closed state, excitation of P; dots, RC in the closed state, excitation of A; long dashes, RC in the open state, excitation of P; solid line, RC in the open state, excitation of A. The transfer equilibrium depends on the state of the RC: in the open state it is shifted to the antenna; in the closed state to the primary donor. (b) Radical pair kinetics in 'native' RCs (solid line) and chromatophores (dashed line) of *Rs. rubrum* calculated with the parameters of Tables 1 and 2 as described in the text. Both kinetics are nearly identical.

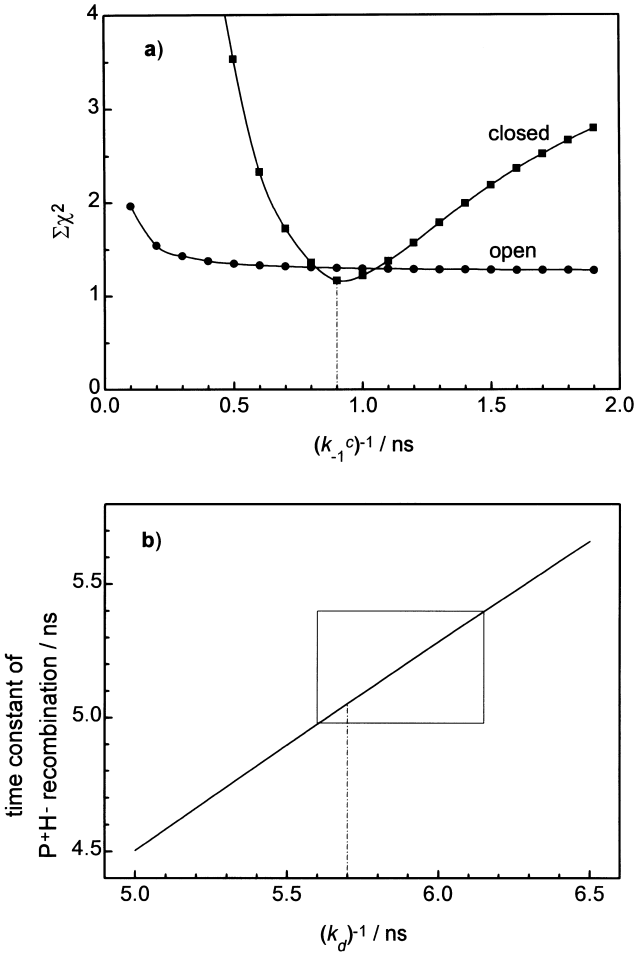

Fig. 4. (a) Dependence of the sum of the squared residuals of the fluorescence signals from *Rs. rubrum* with open (circles) and closed (Q_A^-) (squares) RCs of Fig. 1b on the rate constant of radiative decay of the radical pair, k^c_{-1}. The values of the other parameters (Tables 1 and 2) were held constant. The dash–dot line indicates the selected value of the fit parameter. (b) Dependence of the time constant of P^+H^- recombination for *Rs. rubrum* with closed (Q_A^-) RCs on the rate constant of the radiationless decay of the radical pair, k_d. The values of the other parameters (Tables 1 and 2) were held constant. The box indicates the experimental range reported for the recombination and the resulting range for k_d. The dash–dot line indicates the selected value of the fit parameter.

in the closed state the deviation is less than in the open state. If this model is still used, as for example by Gibasiewicz et al. [31], it remains to be shown that the exciton-radical pair model is a sufficiently good approximation.

4.5. Quality of the fits

Our experimental data in Figs. 1 and 2 were fit with only three adjustable parameters which are the rate constants for: (1) trapping k_t; (2) radiative decay of the radical pair k^c_{-1}; and (3) radiationless decay of the radical pair k_d. In a particular type of experiment, these parameters can compensate each other within a certain range. However, taking into account the constraints, the ranges become very small resulting in a unique set of rate constants (best residuals and fulfilling of the constraints) for each bacterium investigated.

This is illustrated in Fig. 4 for *Rs. rubrum*. The dependence of the sum of squared residuals of the kinetic data (Fig. 1b) on the rate constant of the radiative decay of the radical pair is shown in Fig. 4a. One can see that this rate constant is only well determined by the kinetics from the closed state. The value of k^c_{-1} resulting from this minimum (Fig. 4a) is indicated by the vertical dash-dot lines. Once k^c_{-1} is fixed, the rate constant for the non-radiative decay k_d is confined by the P^+H^--recombination kinetic (5.0–5.4 ns) as shown in Fig. 4b. The analogous figures for *Rsp. viridis* look similar (not shown).

A closer inspection of the kinetic traces in Fig. 1 reveals that the fits are good, but not perfect. As already indicated, this is not due to an experimental insufficiency since better fits could be obtained with other parameters. However, these then come into conflict with the constraints. To explain the small imperfections in the fluorescence decay kinetics we suggest that the reaction scheme (Scheme 1) is too simple. In particular, it does not take into account multiphasic recombination luminescence due to dielectric relaxations in the protein matrix [52–55]. Preliminary fits with a reaction scheme extended by one or two more states (relaxed radical pairs) are capable to produce significantly smaller residuals.

The neglection of radical pair relaxations in our simplified scheme may explain why our calculated F_m/F_o values deviate by 10–20% from the measured ones (see Table 3).

4.6. Escape probabilities

The term 'escape probability' is often intuitively used to quantify the probability of an exciton on the reaction center to jump back into the antenna system instead of driving the primary charge separation. The knowledge of this quantity is of central importance in understanding the trapping mechanism. However, this definition does not allow for a quantitative evaluation of fluorescence excitation spectra.

The escape probability must be independent of whether the exciton is born on P by direct excitation or by transfer from a nearby antenna pigment or by charge recombination. However, for the experimental determination of this quantity the direct excitation of P is required. In this respect, the escape probability is known with reasonable certainty only for those photosystems in which the RC contributes with a distinct absorption band to the total absorption spectrum. This condition is given in LH1-only purple bacteria where the accessory BChls of the RC display a band at approximately 800 nm for *Rs. rubrum* or at 830 nm for *Rsp. viridis* with a height comparable to the antenna pigment absorption. The deviations of the fluorescence excitation spectrum from the (1−T) spectrum then contains the information on the escape probability: if, for example, the escape probability is zero, the RC band is absent in the fluorescence excitation spectrum and if the escape probability is one the fluorescence excitation spectrum matches the (1−T) spectrum. Based on this assay, the escape probabilities of *Rs. rubrum* and *Rps. viridis* have been determined to be very small [10]. In the following, we want to quantify the intermediary cases.

In a strict sense, the escape probability should refer to the physical entity in which the exciton energy is converted either to a photochemical product or to heat. According to this understanding, the probability $p'^{o/c}_{esc}$ (Eq. A5a) may be defined as the probability that the exciton gets lost outside the physical unit of the RC, starting from excitation in the RC. Independent of whether the RCs are open or closed, this probability was calculated to be <0.2 for the two purple bacteria studied (Table 3). Therefore, it is safe to state that a purple bacterial reaction center always represents a trap.

Alternatively, an escape probability may be defined that refers to the locus of fluorescence emission. This leads to the ratio of the antenna fluorescence upon excitation of P to the antenna fluorescence

upon excitation of A, $p''^{o,c}_{esc}$ (Eq. 4b). This definition is equivalent to the ratio of the detrapping rate constant to the sum of the rate constants of detrapping and primary charge separation (Eq. A5b) and has been used by Freiberg et al. [37]. With the numerical values of Tables 1 and 2, these escape probabilities calculate to be $p''^{o}_{esc} = 0.11$ (*Rs. rubrum*) and $p''^{o}_{esc} = 0.37$ (*Rsp. viridis*) for the open state and $p''^{c}_{esc} = 0.57$ (*Rs. rubrum*) and $p''^{c}_{esc} = 0.77$ (*Rsp. viridis*) for the closed (Q_A^-) states. However, this definition is not useful when the fluorescence spectra of P and A strongly overlap, as is the case in purple bacteria.

To quantify the fluorescence excitation spectrum assay one needs a third type of escape probability which takes into account the fluorescence of both, antenna and primary donor according to Eq. A5c. This escape probability, $p^{o/c}_{esc}$, then corresponds to the experimentally accessible quantities. With the numerical values of Tables 1 and 2 the corresponding escape probabilities are $p^{o}_{esc} = 0.14$ (*Rs. rubrum*) and $p^{o}_{esc} = 0.40$ (*Rsp. viridis*) for the open and $p^{c}_{esc} = 0.66$ (*Rs. rubrum*) and $p^{c}_{esc} = 0.79$ (*Rsp. viridis*) for the closed (Q_A^-) state. Our escape probability for *Rs. rubrum* with open RCs of 14% is incompatible with the $25 \pm 5\%$ reported by Timpmann et al. [14] and also our escape probability for *Rsp. viridis* with open RCs of approximately 40% is incompatible with the $\leq 10\%$ reported by Otte et al. [10], but compatible with other references [12,56].

In order to examine the influence of some of the assumptions made on the above conclusions we made computational simulations. First we took into account the possibility that k_{rad} of the P and k_{rad} of A are different. Choosing a k_{rad} of P a factor of two larger or smaller than k_{rad} of A changed the calculated escape propabilities by less than 20% of the values given in Table 3.

Second, we took into consideration that also the accessory BChl (B_A) can initiate charge separation [57,58]. A model calculation with a 4-state kinetic scheme which included B_A as a state was performed. Taking into consideration finite kinetics from B_A* into P* and/or B_A* into radical pair (tested range of time constants 0–6 ps) leaves the contribution of the absorption band of B_A in the fluorescence excitation spectra below $< 2\%$. Hence, the 800-nm band is still below the experimentally detectable level. Therefore, the above quoted escape probabilities are not much effected.

Third, we modeled the influence of the rate constant for non-photochemical losses of P* on our analysis. If we use 200 ps [59–63] instead of 700 ps as the only change the radical pair decay becomes faster by about 10%. However, the effect can be compensated by a similary small change of the rate constant k_d. In summary, this detail neither changes the quality of the fits nor the conclusions. The only changes are slightly different rate constants.

4.7. Photochemical yields

Our parameter set predicts photochemical quantum yields of $> 80\%$ for both bacteria investigated. Although this is a generally accepted value for purple bacteria, in the case of *Rsp. viridis* it is in contrast to reports of about 45% [64,65]. Independent evidence for a high quantum yield in *Rsp. viridis* is given by the binary oscillations of the Q_A^- reoxidation rate [66] which only occur when the quantum yield is high.

4.8. Relation of our model to other models

Models similar to ours have been suggested before [4,11,14,37,67]. However, they were not rigorously used for data analysis. Either decay paths were neglected or the violation of experimentally well-established constraints was not tested.

Theoretically, if detrapping is not negligible, the molecular time constant for trapping can be significantly different from the measured decay time constant. In some cases the observed decay times have been converted into molecular rate constants assuming a particular model. For instance, for *Rs. rubrum* Timpmann and colleagues [4,14] concluded from a 69-ps measured decay time on a 35-ps molecular time constant which is incompatible with our analysis. The reason for this discrepancy is a two-fold neglection, both of losses from the antenna and of radiationless decay paths of the radical pair.

4.9. Recombination kinetics

The recombination of the radical pair consist of two main paths: formation of P* and ground (or

triplet) state formation. The corresponding rate constants are listed in Table 2. In both bacteria, the radiative backreaction is significantly faster than the radiationless recombination. The rate constant of the radiative backreaction of the radical pair k^c_{-1} is larger for *Rs. rubrum* $(0.9\ \text{ns})^{-1}$ than for *Rsp. viridis* $(1.5\ \text{ns})^{-1}$, whereas the radiationless recombination rate constant k_d is smaller for *Rs. rubrum* $(5.7\ \text{ns})^{-1}$ than for *Rsp. viridis* $(3.15\ \text{ns})^{-1}$. These data indicate marked differences between the RCs of BChl *a*- and BChl *b*-containing bacteria.

4.10. Trapping mechanism in purple bacteria

In the transfer-to-the-trap-limited mechanism the rate-limiting step is the exciton transfer from the antenna to the primary donor, which means that the backtransfer to the antenna does not compete with the primary charge separation. The trapping kinetic is then hardly influenced by the speed of the primary charge separation. On the other hand, if the speed of the primary charge separation controls the trapping time one speaks about trap-limited or RC-controlled energy capture.

In the case of *Rs. rubrum*, the about two-fold slower primary charge separation in closed RC slows down the trapping time from 68 to 73 ps (Table 4). This small 7% effect classifies the trapping mechanism in this purple bacterium – and probably all other ones with similar spectral properties – to the transfer-to-the-trap-limited mechanism. In the case of *Rps. viridis*, however, the two-fold slower primary charge separation in closed RCs slows down the trapping time from 69 to 91 ps (Table 4) or from 60 to 90 ps [12]. This 32% effect (or 50% [12]) classifies the trapping mechanism in *Rps. viridis* to be in between the transfer-to-the-trap- and trap-limited mechanism.

4.11. Fluorescence from the primary donor

Our analysis was performed under the assumption of equal radiative rate constants from the antenna and the primary donor. The model then predicts that, independent of the trapping mechanism, the fluorescence from the primary donor to be smaller than the fluorescence from the antenna, no matter whether the excitation occurs in A or P and no matter whether the RCs are open or closed (Table 3). Specifically, in the case *Rs. rubrum* with open RCs the fraction of fluorescence from P to the overall fluorescence is <0.04 or <0.28 depending on excitation in A or P, respectively. In the case of closed RCs the fraction of fluorescence from P to the overall fluorescence is <0.17 or <0.28, again depending on excitation in A or P, respectively. In the case of *Rsp. viridis* with open RCs the fraction of fluorescence from P to the overall fluorescence is <0.04 or <0.09 depending on excitation in A or P, respectively. In the case of closed RCs, the fraction of fluorescence to the overall fluorescence is <0.07 or <0.09, again depending on excitation in A or P, respectively. If k_{rad} of P is different from k_{rad} of A the fluorescence yields of P change in direct proportion (Eq. A4b). Since k_{rad} of P is not known these results remain correspondingly uncertain.

The lower emission from P* in *Rsp. viridis* compared to *Rs. rubrum* when the RCs are closed (Q_A^-) is directly related to the higher escape probabilities in *Rsp. viridis*. Therefore, the extent of the 'extensive energy transfer' from the reaction center to the antenna in the closed case proposed by Otte et al. [10] is larger in BChl *b* containing purple bacteria than in BChl *a* containing ones.

4.12. Comparison of native RC and RC preparations

The properties of the hypothetically isolated RC ('native' RC) can be modeled straightforwardly by omitting the antenna, trapping and detrapping (Scheme 1). The simulated kinetics of the P^+H^--recombination under reducing conditions for both, 'native' RCs and chromatophores, are shown in Fig. 3b for *Rs. rubrum*. The decay kinetics (apparent time constants of 5.05 ns (chromatophores) and 5.50 ns ('native' RCs); Table 4) of the two traces look very similar. This is particularly true when the traces are normalized to their maximum and convoluted with a 1 ns apparatus response function, to simulate real experimental conditions (not shown). The figure for *Rps. viridis* was similar. The apparent decay time constants were 2.80 and 3.11 ns, respectively (Table 4). The numbers for the chromatophore systems agree reasonably well with the published values of about 5 ns from *Rb. sphaeroides* and 2.8 ns from *Rsp. viridis* [30,31]. In summary, the differences in

decay kinetics between the antenna systems and RCs do not exceed 10%.

In contrast to the above theoretical predictions, the experimental kinetics seem to depend significantly on the preparation. In RC preparations, the charge recombination is found to be in the 5–15 ns range [52,54], whereas in membranes, it is in the 3–6 ns range [30,31] but only in [30,31] a direct comparison was made. Measurements with chromatophores of antenna deficient strains of *Rb. sphaeroides* show that the rate constant of the primary charge separation is up to 30% slower in detergent preparations than in chromatophores of the same strain [68]. Two possible explanations were considered by Gibasiewicz and coworkers to explain the difference in the P^+H^--recombination kinetics [30,31]: either (1) a modification of the RC properties by the detergent used for the preparation; or (2) the backtransfer of the excited state to the antenna which makes up the essential difference between the two samples. According to our model calculations (Fig. 3b), this latter explanation can be excluded, making the detergent modification hypothesis the more likely explanation. However, there is a third possibility, namely an influence of the LH1-complex on the RC which results in a lowered redox potential of the primary donor [68].

5. Conclusions

A three-state model for the core complexes of purple bacteria is sufficient to account for all main experimental data. A unique set of the molecular rate constants involved was determined from the experimentally given constraints. In the framework of the model (Scheme 1) and the rate constants (Tables 1 and 2) the following conclusions can be drawn:

- The trapping mechanism in *Rs. rubrum* is transfer-to-the-trap-limited, whereas in *Rsp. viridis*, it is between the transfer-to-the-trap-limited and trap-limited one.
- The molecular rate constant for trapping is (69 ps)$^{-1}$ for *Rs. rubrum* and (52 ps)$^{-1}$ for *Rsp. viridis*.
- The molecular rate constant for the radiative back-reaction in closed (Q_A^-) RCs is (900 ps)$^{-1}$ for *Rs. rubrum* and (1 500 ps)$^{-1}$ for *Rsp. viridis*.
- In closed (Q_A^-) RCs, the deactivation of the radical pair into the ground state cannot be neglected. Its rate constant is (5–6 ns)$^{-1}$ in *Rs. rubrum* and (3–3.5 ns)$^{-1}$ in *Rsp. viridis*.
- The escape probability, as defined by the ratio of the total fluorescence yields upon selective excitation of P compared to excitation of A, is $\approx$14% in *Rs. rubrum* with open RCs and $\approx$66% with closed RCs. For *Rps. viridis* the numbers are $\approx$40% and $\approx$79%, respectively.
- The P^+H^--recombination kinetics in closed (Q_A^-) RCs is mainly determined by the radiationless decay of the radical pair. This kinetics are only slightly dependent on the presence or absence of antenna pigments.

Acknowledgements

The authors thank Dr. K. Brettel and Dr. W. Leibl for valuable discussions and experimental support. The work was financially supported by the Deutsche Forschungsgemeinschaft (SFB 171-A1).

Appendix A

Scheme 1 can be described by a set of ODEs whose rate matrix reads:

$$T = \begin{vmatrix} -(k_\ell + k_t) & k_{-t} & 0 \\ k_t & -(k_1^{o,c} + k_{-t} + k_\ell) & k_{-1} \\ 0 & k_1{}^{o,c} & -(k_2 + k_{-1} + k_d) \end{vmatrix} \quad \text{(A1)}$$

The matrix was solved for the two extreme initial conditions, namely excitation into the antenna:

$$z_0 = \begin{vmatrix} 1 \\ 0 \\ 0 \end{vmatrix} \quad \text{(A2a)}$$

and excitation of the primary donor:

$$z_0 = \begin{vmatrix} 0 \\ 1 \\ 0 \end{vmatrix} \quad \text{(A2b)}$$

where z_0 describes the initial exciton density.

The solution of this set of ODEs consists of a sum over three exponential functions whose time constants, τ_i, are the reciprocal eigenvalues of the rate matrix (Eq. A1). The prefactors, a_i, follow from the eigenvectors of the rate matrix (Eq. A1) and the initial condition (e.g. [69]). This yields the kinetics of the excited antenna state $A(t)$, the excited primary donor $P(t)$ and the radical pair RP(t). The overall fluorescence decay kinetics is proportional to k_{rad} and to the excited state kinetics:

$$F(t) = k_{rad}A(t) + k_{rad}P(t) \tag{A3}$$

The overall radiative emission from A* and P* upon excitation in A for the open and closed (Q_A^-) state (${}^{A}F_A^{o,c}$,${}^{A}F_P^{o,c}$) and the emission from A* and P* upon excitation in P for the open and closed (Q_A^-) state (${}^{P}F_A^{o,c}$,${}^{P}F_P^{o,c}$) are obtained by integration of $A(t)$ and $P(t)$, calculated for the particular excitation and redox conditions:

$${}^{A,P}F_A^{o,c} = k_{rad}\int_0^\infty A(t)\mathrm{d}t, \tag{A4a}$$

$${}^{A,P}F_P^{o,c} = k_{rad}\int_0^\infty P(t)\mathrm{d}t. \tag{A4b}$$

The escape probability may be defined differently. Three definitions shall be inspected in more detail which all relate to exciton creation in P. First, the escape probability may be defined as the probability that the exciton does not get lost anywhere in the physical unit of the RC. If the total decay probability is 1:

$$p'^{o,c}_{esc} = 1 - (k_d + k_2)\int_0^\infty \mathrm{RP}(t)\mathrm{d}t. \tag{A5a}$$

In the case of the closed (Q_A^-) state, k_2 is set to zero.

Second, the escape probability may be defined as the ratio of the antenna fluorescence upon excitation of P to the antenna fluorescence upon excitation of A

$$p''^{o,c}_{esc} = \frac{{}^{P}F_A^{o,c}}{{}^{A}F_A^{o,c}} = \frac{k_{-t}}{k_{-t} + k_1}. \tag{A5b}$$

It can be shown by means of the analytical solutions for the fluorescence yields that this quotient corresponds to the ratio of the detrapping rate constant to the sum of the rate constants of detrapping and primary charge separation.

Finally, a third type of escape probability may be defined which takes into account both fluorescence yields:

$$p^{o,c}_{esc} = \frac{{}^{P}F_A^{o,c} + {}^{P}F_P^{o,c}}{{}^{A}F_A^{o,c} + {}^{A}F_P^{o,c}} \tag{A5c}$$

The equilibration kinetics shall by defined by the ratio of $P(t)$ and $A(t)$

$$\tilde{K}^{o,c}(t) = \frac{P^{o,c}(t)}{A^{o,c}(t)} \tag{A6}$$

and the transfer equilibrium constant follows by

$$\tilde{K}_0^{o,c} = \tilde{K}^{o,c}\ (t \to \infty). \tag{A7}$$

References

[1] M.Z. Papiz, S.M. Prince, A.M. Hawthornthwaite, G. McDermott, A.A. Freer, N.W. Isaacs, R.J. Cogdell, Trends Plant Sci. 1 (1996) 198–206.

[2] R. van Grondelle, J.P. Dekker, T. Gillbro, V. Sundström, Biochim. Biophys. Acta 1187 (1994) 1–65.

[3] V. Sundström, R. van Grondelle, in: R.E. Blankenship, M.T. Madigan, C.E. Bauer (Eds.), Anoxygenic Photosynthetic Bacteria, Kluwer Academic Publishers, Dordrecht, 1995, pp. 349–372.

[4] A. Freiberg, in: R.E. Blankenship, M.T. Madigan, C.E. Bauer (Eds.), Anoxygenic Photosynthetic Bacteria, Kluwer Academic Publishers, Dordrecht, 1995, pp. 385–386.

[5] M.G. Müller, G. Drews, A.R. Holzwarth, Biochim. Biophys. Acta 1142 (1993) 49–58.

[6] A.Y. Borisov, Photosynth. Res. 23 (1990) 283–289.

[7] S. Karrasch, P.A. Bullough, R. Ghosh, EMBO J. 14 (1995) 631–638.

[8] F.A.M. Kleinherenbrink, G. Deinum, S.C.M. Otte, A.J. Hoff, J. Amesz, Biochim. Biophys. Acta 1099 (1992) 175–181.

[9] A.S. Holt, R.K. Clayton, Photochem. Photobiol. 4 (1965) 829–831.

[10] S.C.M. Otte, F.A.M. Kleinherenbrink, J. Amesz, Biochim. Biophys. Acta 1143 (1993) 84–90.

[11] W.H. Xiao, S. Lin, A.K.W. Taguchi, N.W. Woodbury, Biochemistry 33 (1994) 8313–8322.

[12] F.G. Zhang, T. Gillbro, R. van Grondelle, V. Sundström, Biophys. J. 61 (1992) 694–703.

[13] K. Timpmann, A. Freiberg, V. Sundström, Chem. Phys. 194 (1995) 275–283.

[14] K. Timpmann, F.G. Zhang, A. Freiberg, V. Sundström, Biochim. Biophys. Acta 1183 (1993) 185–193.
[15] I.A. Abdourakhmanov, R.V. Danielius, A.P. Razjivin, FEBS Lett. 245 (1989) 47–50.
[16] A.P. Razjivin, R.V. Danielius, R.A. Gadonas, A.Y. Borisov, A.S. Piskarskas, FEBS Lett. 143 (1982) 40–44.
[17] T.G. Monger, R.J. Cogdell, W.W. Parson, Biochim. Biophys. Acta 449 (1976) 136–153.
[18] K. Timpmann, A. Freiberg, V.I. Godik, Chem. Phys. Lett. 182 (1991) 617–622.
[19] E. Bittersmann, R.E. Blankenship, N.W. Woodbury, in: M. Baltscheffsky (Ed.), Current Research in Photosynthesis, Kluwer Academic Publishers, Dordrecht, 1990, pp. 169–172.
[20] V. Sundström, R. van Grondelle, J. Photochem. Photobiol. B 15 (1992) 141–150.
[21] F.A.M. Kleinherenbrink, P. Cheng, J. Amesz, R.E. Blankenship, Photochem. Photobiol. 57 (1993) 13–18.
[22] A.Y. Borisov, V.I. Godik, K.K. Rebane, K.E. Timpmann, Biochim. Biophys. Acta 807 (1985) 221–229.
[23] H.-W. Trissl, J. Breton, J. Deprez, A. Dobek, W. Leibl, Biochim. Biophys. Acta 1015 (1990) 322–333.
[24] H. Kingma, L.N.M. Duysens, R. van Grondelle, Biochim. Biophys. Acta 725 (1983) 434–443.
[25] H.-W. Trissl, Photosynth. Res. 47 (1996) 175–185.
[26] P. Hamm, K.A. Gray, D. Oesterhelt, R. Feick, H. Scheer, W. Zinth, Biochim. Biophys. Acta 1142 (1993) 99–105.
[27] J. Breton, J.-L. Martin, A. Migus, A. Antonetti, A. Orszag, Proc. Natl. Acad. Sci. USA 83 (1986) 5121–5125.
[28] W. Holzapfel, U. Finkele, W. Kaiser, D. Oesterhelt, H. Scheer, H.U. Stilz, W. Zinth, Proc. Natl. Acad. Sci. USA 87 (1990) 5168–5172.
[29] M.R. Wasielewski, D.M. Tiede, FEBS Lett. 204 (1986) 368–372.
[30] K. Gibasiewics, K. Brettel, A. Dobek, W. Leibl, in: Photosynthesis: Mechanisms and Effects. Proceedings of the XIth International Congress on Photosynthesis, G. Garab (Ed.), Kluwer Academic Publishers, Dordrecht, 1998, pp. 841–844.
[31] K. Gibasiewics, K. Brettel, A. Dobek, W. Leibl, Chem. Phys. Lett. 315 (2000) 95–102.
[32] R.W. Visschers, S.I.E. Vulto, M.R. Jones, R. van Grondelle, R. Kraayenhof, Photosynth. Res. 59 (1999) 95–104.
[33] G. Drews, Mikrobiologisches Praktikum, Springer Verlag, Berlin, 1983.
[34] H.-W. Trissl, K. Wulf, Biospectroscopy 1 (1995) 71–82.
[35] V.A. Shuvalov, W.W. Parson, Proc. Natl. Acad. Sci. USA 78 (1981) 957–961.
[36] A.R. Holzwarth, in: J. Amesz, A.J. Hoff (Eds.), Biophysical Techniques in Photosynthesis, Kluwer Academic Press, Dordrecht, 1996, pp. 75–92.
[37] A. Freiberg, J.P. Allen, J.C. Williams, N.W. Woodbury, Photosynth. Res. 48 (1996) 309–319.
[38] T. Walz, R. Ghosh, J. Mol. Biol. 265 (1997) 107–111.
[39] P.O.J. Scherer, S.F. Fischer, J.K.H. Hörber, M.E. Michel-Beyerle, H. Michel, M.E. Michel-Beyerle (Ed.), in: Antennas and Reaction Centers of Photosynthetic Bacteria, Springer-Verlag, Berlin, 1985, pp. 131–137.
[40] K.R. Miller, Nature 300 (1982) 53–55.
[41] M.H. Vos, F. Rappaport, J.-C. Lambry, J. Breton, J.-L. Martin, Nature 363 (1993) 320–325.
[42] W. Zinth, M.C. Nuss, M.A. Franz, W. Kaiser, H. Michel, in: M.E. Michel-Beyerle (Ed.), Antennas and Reaction Centers of Photosynthetic Bacteria, Springer-Verlag, Berlin, 1985, pp. 286–291.
[43] I.H.M. van Stokkum, L.M.P. Beekman, M.R. Jones, M.E. van Brederode, R. van Grondelle, Biochemistry 36 (1997) 11360–11368.
[44] V.Z. Paschenko, V.V. Gorokhov, N.P. Grishanova, E.A. Goryacheva, B.N. Korvatovsky, P.P. Knox, N.I. Zakharova, A.B. Rubin, Biochim. Biophys. Acta 1364 (1998) 361–372.
[45] P. Hamm, M. Zurek, W. Mäntele, M. Meyer, H. Scheer, W. Zinth, Proc. Natl. Acad. Sci. USA 92 (1995) 1826–1830.
[46] J. Deprez, H.-W. Trissl, J. Breton, Proc. Natl. Acad. Sci. USA 83 (1986) 1699–1703.
[47] M.G. Rockley, M.W. Windsor, R.J. Cogdell, W.W. Parson, Proc. Natl. Acad. Sci. USA 72 (1975) 2251–2255.
[48] V. Jirsakova, F. Reisshusson, J.L. Ranck, I. Moya, Photosynth. Res. 54 (1997) 35–43.
[49] K. Bernhardt, H.-W. Trissl, Biochim. Biophys. Acta 1409 (1999) 125–142.
[50] T. Ritz, X. Hu, A. Damjanovic, K. Schulten, J. Lumin. 76/77 (1998) 310–321.
[51] L.M.P. Beekman, F. van Mourik, M.R. Jones, H.M. Visser, C.N. Hunter, R. van Grondelle, Biochemistry 33 (1994) 3143–3147.
[52] J.M. Peloquin, J.C. Williams, X.M. Lin, R.G. Alden, A.K.W. Taguchi, J.P. Allen, N.W. Woodbury, Biochemistry 33 (1994) 8089–8100.
[53] N.W. Woodbury, J.M. Peloquin, R.G. Alden, X.M. Lin, S. Lin, A.K.W. Taguchi, J.C. Williams, J.P. Allen, Biochemistry 33 (1994) 8101–8112.
[54] N.W. Woodbury, W.W. Parson, Biochim. Biophys. Acta 767 (1984) 345–361.
[55] N.W. Woodbury, W.W. Parson, M.R. Gunner, R.C. Prince, P.L. Dutton, Biochim. Biophys. Acta 851 (1986) 6–22.
[56] A. Osyczka, K.V.P. Nagashima, S. Sogabe, K. Miki, M. Yoshida, K. Shimada, K. Matsuura, Biochemistry 37 (1998) 11732–11744.
[57] M.E. van Brederode, M.R. Jones, F. van Mourik, I.H.M. van Stokkum, R. van Grondelle, Biochemistry 36 (1997) 6855–6861.
[58] M.E. van Brederode, F. van Mourik, I.H.M. van Stokkum, M.R. Jones, R. van Grondelle, Proc. Natl. Acad. Sci. USA 96 (1999) 2054–2059.
[59] D. Holten, M.W. Windsor, W.W. Parson, J.P. Thornber, Biochim. Biophys. Acta 501 (1978) 112–126.
[60] A.K.W. Taguchi, J.W. Stocker, R.G. Alden, T.P. Causgrove, J.M. Peloquin, S.G. Boxer, N.W. Woodbury, Biochemistry 31 (1992) 10345–10355.

[61] J. Breton, J.-L. Martin, J.-C. Lambry, S.J. Robles, D.C. Youvan, in: M.E. Michel-Beyerle (Ed.), Reaction Centers of Photosynthetic Bacteria, Springer-Verlag, Berlin, 1990, pp. 293–302.
[62] M.H. Vos, J.-C. Lambry, S.J. Robles, D.C. Youvan, J. Breton, J.-L. Martin, Proc. Natl. Acad. Sci. USA 88 (1991) 8885–8889.
[63] H. Kramer, G. Deinum, A.T. Gardiner, R.J. Cogdell, C. Francke, T.J. Aartsma, J. Amesz, Biochim. Biophys. Acta 1231 (1995) 33–40.
[64] R.P. Carithers, W.W. Parson, Biochim. Biophys. Acta 387 (1975) 194–211.
[65] J.P. Thornber, J.M. Olson, Photochem. Photobiol. 14 (1971) 329–341.
[66] W. Leibl, J. Breton, Biochemistry 30 (1991) 9634–9642.
[67] B. Källebring, Ö. Hansson, Chem. Phys. 149 (1991) 361–372.
[68] L.M.P. Beekman, R.W. Visschers, R. Monshouwer, M. Heerdawson, T.A. Mattioli, P. McGlynn, C.N. Hunter, B. Robert, I.H.M. van Stokkum, R. van Grondelle, M.R. Jones, Biochemistry 34 (1995) 14712–14721.
[69] P.D. Laible, W. Zipfel, T.G. Owens, Biophys. J. 66 (1994) 844–860.